

to be 26% of the total yield at 1 MeV for a 2-mm-thick silicon crystal. The yields due to Coulomb scattering were determined by integrating the Gaussian peak and correcting for the yield in the low-energy tail.

The experimental cross sections  $d\sigma/d\Omega$  were reduced from the measured yields by use of the following relation:

$$d\sigma/d\Omega = N/\Delta\Omega qt.$$

The quantity  $N$  is the yield of electrons measured in a known solid angle  $\Delta\Omega$  at a given scattering angle. The quantity  $t$  is the number of target atoms per  $\text{cm}^2$  normal to the beam direction and is determined from the target thickness. The quantity  $q$  is the number of electrons incident on the target.

The measured cross sections were compared to the Mott cross sections which were calculated by Doggett and Spencer.<sup>2</sup> These comparisons are shown in Fig. 4 where the differential cross section  $d\sigma/d\Omega$  for Coulomb scattering without atomic excitation, normalized to the

Rutherford cross section  $d\sigma/d\Omega_R$ , is plotted as a function of scattering angle. The calculations of Doggett and Spencer have neglected finite nuclear size and atomic electron screening, since they have negligible effect for aluminum at the values of momentum transfer for which the cross sections were determined. The present experimental values are, on the average, 8% lower than the theoretical values at scattering angles 90 deg and smaller, while the experimental values for angles greater than 90 deg are on the average less than 3% lower. The results reported by Spiegel *et al.*,<sup>1</sup> using a magnetic spectrometer and a 1.5-mg/cm<sup>2</sup> Al target at 1 MeV, on the other hand, are lower than the Mott cross section values by an average of 3% at the forward angles, while the values at backward angles are about 10% below the Mott cross sections. Although the apparent shape of each of the experimental cross-section curves differs from the shape of the Mott cross-section curve, both measurements confirm the Mott cross sections within the estimated experimental errors.

## Absolute Total Electron-Helium-Atom Scattering Cross Sections for Low Electron Energies\*

D. E. GOLDEN AND H. W. BANDEL

Research Laboratories, Lockheed Missiles & Space Company, Palo Alto, California

(Received 6 November 1964)

The Ramsauer technique has been used to measure the absolute total electron-helium-atom scattering cross section as a function of electron energy from 0.30 to 28 eV with an estimated probable error of  $\pm 3\%$ . No "fine structure" has been observed at the lower electron energies studied. The variation of the cross section with energy for energies less than 3 eV is in reasonable agreement with the modified effective-range formula given by O'Malley, using a scattering length of  $1.15a_0$ . The cross section first increases with decreasing electron energy from  $2.2 \text{ \AA}^2$  at 28.0 eV to a maximum of  $5.6 \text{ \AA}^2$  at about 1.2 eV and then decreases to  $5.4 \text{ \AA}^2$  at 0.300 eV. The cross section has been found to decrease sharply with increasing energy at about 0.5 eV below the first excitation energy. This resonance, predicted by Baranger and Gerjuoy and originally observed by Schulz, first decreases with increasing energy to a minimum of about 10% below the background at  $19.285 \pm 0.025$  eV and then increases to a gentle maximum of about 3% above the background at  $19.65 \pm 0.05$  eV. The resolution of this resonance as well as the 10% decrease in the cross section at the minimum is determined by the half-width of the electron beam at this energy which is about 0.1 eV.

### INTRODUCTION

THE earliest direct measurements of the total electron-rare-gas atom scattering cross section which attempted to use electrons of well-defined energy were made by Ramsauer<sup>1</sup> in 1921. These measurements were extended by Brode<sup>2</sup> in 1925, who used a slightly different technique.

For helium,<sup>3</sup> Brode's results<sup>2</sup> are in general about 25%

lower than Ramsauer's.<sup>1,4</sup> The total cross section was calculated by Allis and Morse<sup>5</sup> in 1931 by using a simple atomic model. McDougall,<sup>6</sup> shortly thereafter, calculated the cross section by considering a Hartree field due to the atom and making a partial-wave analysis for the ( $l=0, 1, 2,$ ) partial waves. McDougall's calculation yielded a cross section which is about 17% lower than Brode's measurement at 25 eV. The two results agree at about 17 eV and McDougall's results are considerably higher, even than Ramsauer's at lower energies. By

\* Supported by the Lockheed Independent Research Program.

<sup>1</sup> C. Ramsauer, Ann. Physik **66**, 546 (1921), measured the total cross section in helium for electron energies from about 1 to 50 eV.

<sup>2</sup> R. B. Brode, Phys. Rev. **25**, 636 (1925).

<sup>3</sup> Throughout this paper, the discussion will always be about helium, except where specifically mentioned otherwise.

<sup>4</sup> However, Brode's and Ramsauer's results are approximately the same at about 3.75 eV.

<sup>5</sup> W. P. Allis and P. M. Morse, Z. Physik **70**, 567 (1931).

<sup>6</sup> J. McDougall, Proc. Roy. Soc. (London) **A136**, 549 (1932).

including electron exchange, Morse and Allis<sup>7</sup> improved McDougall's partial-wave analysis for the ( $l=0, 1$ ) partial waves. These calculations agree within a few percent with the results of Brode for electron energies greater than about 6 eV. However, for 1 eV these results are significantly larger than Ramsauer's. There were other early measurements of the total cross section which were mainly involved with extending the measurements to lower electron energies,<sup>8-10</sup> but, in the thirties the cross section was certainly not known to better than about 25%. From the thirties to the fifties there seems to be no further experimental or theoretical work on this problem.

Starting with the microwave method developed at MIT<sup>11</sup> in 1951 for the measurement of the cross section for momentum transfer, many indirect cross-section measurements have been made.<sup>12-17</sup> All of these indirect measurements, which are mainly concerned with extremely low energies, agree within about 45% with the exception of Ref. 17, which gives results that are as much as a factor of 3 larger than those of the other indirect measurements at 0.19 eV. The latest low-energy calculations are even in poorer agreement at zero energy.<sup>18-21</sup>

For the electron-atom cross-section measurements described in this paper, the electrons are momentum-selected in order to obtain electrons of well-defined energy and then are allowed to interact with the gas studied. The cross section is directly determined by a study of the beam attenuation as a function of gas pressure. It is believed that precise direct measurements which cover the region from very low energies to moderate energies will give insight into the differences between various previous electron-helium-atom scattering cross sections.

#### APPARATUS

A schematic diagram of the experimental apparatus is shown in Fig. 1. The chamber which is of all-metal construction may be connected through a molecular-sieve trap<sup>22</sup> to a water baffle and then to a standard 2-in.

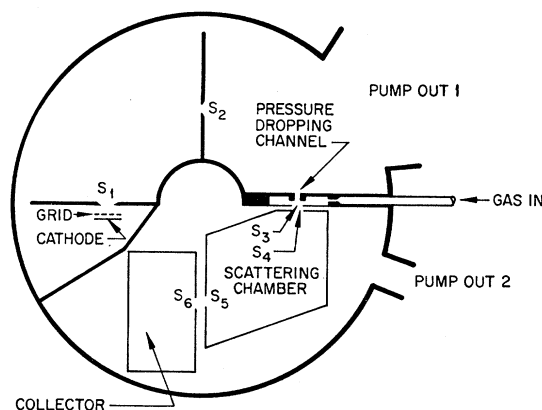


FIG. 1. The experimental arrangement.

oil diffusion pump. This apparatus is part of a bakeable system which is capable of an ultimate pressure of less than  $10^{-9}$  Torr. The rate of rise of pressure when the system is blanked off from the pump is about  $2 \times 10^{-9}$  Torr/min in the first 5 min. For the present measurements, the metal parts of the chamber which are visible to the electron beam have been sprayed with a dispersion of colloidal graphite in order to eliminate contact potential differences between various parts.<sup>23</sup>

The whole apparatus is placed in a uniform magnetic field perpendicular to the plane of the diagram. Electrons from an indirectly heated cathode are accelerated by a negative voltage on it with respect to the rest of the apparatus, which is grounded. The control grid is made of 0.001-in.-diam tungsten wires about 0.01 in. apart and transverse to the long dimension of the slit. It is operated either positive or negative with respect to the cathode, as needed to obtain suitable currents and beam conditions. The electrons are momentum selected by a  $180^\circ$  selection region consisting of the three grounded slits S<sub>1</sub>, S<sub>2</sub>, and S<sub>3</sub>. There are also baffles throughout the selection region (not shown) to cut down the possibility of low-energy electrons bouncing around the apparatus and on through the slit system. After the electrons pass through the selection region, they pass through a  $90^\circ$  scattering region, and then into a collector. The cathode and selection regions may be pumped separately from the rest of the chamber. This allows gas to be maintained in the scattering region while the cathode and selection regions are under vacuum. Equilibrium is then obtained by balancing the rate of gas inflow to the scattering region with the rate of outflow through the pressure-dropping channel. Such differential pumping allows the use of higher pressures in the scattering region by preventing different rates of gas cooling of the cathode surface for different gas pressures. It also allows lower energy electron beams by reducing background scattering in the selection region.

<sup>23</sup> J. H. Parker and R. W. Warren, *Rev. Sci. Instr.* **33**, 948 (1962).

<sup>7</sup> P. M. Morse and W. P. Allis, *Phys. Rev.* **44**, 269 (1933).

<sup>8</sup> E. Brüche, *Ann. Physik* **84**, 279 (1927).

<sup>9</sup> C. Ramsauer and R. Kollath, *Ann. Physik* **3**, 536 (1929), measured the total cross section in helium for electron energies from about 0.2 to 2.2 eV.

<sup>10</sup> C. E. Norman, *Phys. Rev.* **35**, 1217 (1930).

<sup>11</sup> A. V. Phelps, O. T. Fundingsland, and S. C. Brown, *Phys. Rev.* **84**, 559 (1951).

<sup>12</sup> L. Gould and S. C. Brown, *Phys. Rev.* **95**, 897 (1954).

<sup>13</sup> J. M. Anderson and L. Goldstein, *Phys. Rev.* **102**, 388 (1956).

<sup>14</sup> A. V. Phelps, J. L. Pack, and L. S. Frost, *Phys. Rev.* **117**, 470 (1960).

<sup>15</sup> J. C. Bowe, *Phys. Rev.* **117**, 1416 (1960).

<sup>16</sup> L. S. Frost and A. V. Phelps, *Phys. Rev.* **136**, A1538 (1964).

<sup>17</sup> E. M. Bulewicz, *J. Chem. Phys.* **36**, 385 (1962).

<sup>18</sup> B. Kivel, *Phys. Rev.* **116**, 1484 (1959).

<sup>19</sup> B. L. Moisewitsch, *Proc. Roy. Soc. (London)* **77**, 721 (1961).

<sup>20</sup> T. F. O'Malley, *Phys. Rev.* **130**, 1020 (1963).

<sup>21</sup> Y. V. Martynenko, O. B. Firsoy, and M. I. Chibisov, *Zh. Eksperim. i Teor. Fiz.* **44**, 225 (1963) [English transl.: *Soviet Phys.—JETP* **17**, 154 (1963)].

<sup>22</sup> M. A. Biondi, *Rev. Sci. Instr.* **30**, 831 (1959).

The following dimensions are given in centimeters. The mean radius of the electron beam in the apparatus is 2.5. For the present work the slits were as follows:  $S_1=S_2=0.091 \times 0.500$ ,  $S_3=0.076 \times 0.500$ ,  $S_4=0.159 \times 0.599$ ,  $S_5=S_6=0.401 \times 1.198$ . The pressure-dropping channel begins 0.035 from the face of  $S_3$  and extend about 0.52 back along the curved path of the beam; its cross section is  $0.091 \times 0.515$ .

The pressure in the scattering region was measured by a Schulz-Phelps high-pressure ion gauge,<sup>24</sup> which was calibrated by means of a capacitance manometer attached to the system and connected to two McLeod gauges.<sup>25</sup> Such an arrangement was used in order to prevent mercury contamination of the apparatus. The ion gauges appeared to be quite reliable when calibrated after bakeout. Accuracy of the McLeod gauges was  $\pm 1\%$ . Zero drift of the capacitance manometer and reading errors introduce an additional error of about  $\pm 2\%$ .

The currents to the scattering chamber and electron collector were measured by vibrating-reed electrometers which allowed the measurement of currents while maintaining both chambers at ground potential within a very close tolerance. Signal resistors in the two electrometers were compared in pairs several times during the course of the work, and corrections accurate to about  $\pm 0.1\%$  were made for their differences; absolute calibrations were not needed, because only ratios of currents enter into the cross-section determination. Over-all behavior of the electrometers was checked by comparing measured input and output voltages, and was accurate to about  $\pm 0.3\%$  at their outputs. All voltages were measured with a precision differential dc voltmeter.

### PROCEDURE

If it is assumed that a current of electrons  $I_{c0}+I_{s0}=I_0$  enters the scattering region, then the current reaching the collector is given by

$$I_c = I_{c0} \exp(-\sigma n x), \quad (1)$$

where  $I_{c0}$  is that part of the current entering the scattering region which will reach the collector at zero pressure,  $\sigma_s$  is the total cross section,  $n$  is the gas density, and  $x$  is the path length of the electron beam through the scattering chamber. The current reaching the scattering chamber is given by

$$I_s = I_{s0} + I_{c0}[1 - \exp(-\sigma n x)], \quad (2)$$

where  $I_{s0}$  is that part of the current entering the scattering region which will reach the scattering chamber at zero pressure. Equations (1) and (2) may be combined into

$$\ln[(I_c + I_s)/I_c] = \ln[(I_{c0} + I_{s0})/I_{c0}] + \sigma n x. \quad (3)$$

<sup>24</sup> G. J. Schulz and A. V. Phelps, Rev. Sci. Instr. 28, 1051 (1957).

<sup>25</sup> The sensitivity to helium was measured to be  $0.06 \text{ Torr}^{-1}$  by using helium in the experimental chamber and either helium or argon in the McLeod gauge.

This equation may be rewritten as

$$\ln F = \ln F_0 + \sigma n x. \quad (4)$$

Hence, at constant electron energy and constant  $F_0$ , the slope of a plot of  $\ln F$  versus gas density, or pressure at constant temperature, yields the cross section at that energy.<sup>26</sup> The method of measurement described above is essentially the same as that used by Ramsauer<sup>1</sup> with the addition of the provision here for differential pumping. Brode's<sup>2</sup> apparatus was a modification of Ramsauer's. Instead of separate selection and scattering regions, Brode used the same region for selecting and scattering. In the present experimental arrangement, this can be accomplished by connecting the scattering chamber to the collector and using the region between  $S_1$  and  $S_3$  as the scattering region. In such a case, it must be assumed that the current passing through  $S_3$  from the cathode is proportional to the current leaving the cathode. Once this is done, Eq. (4) may again be used. However,  $F$  and  $F_0$  must be reinterpreted as  $[I_k/(I_c + I_s)]$  and  $[I_{k0}/(I_{c0} + I_{s0})]$ , where  $I_k$  is the current leaving the cathode,  $I_{k0}$  is the current leaving the cathode at zero pressure which must be assumed equal to  $I_c$ , and  $x$  must be reinterpreted as the path length of the electron beam between  $S_1$  and  $S_3$ .

At the outset, in order to look for differences between the Brode and Ramsauer methods, by means of a switching arrangement, both types of signal were measured at the same time as a function of accelerating voltage at constant grid voltage  $V_g=0$ , constant magnetic field strength, and constant heat to the cathode in vacuum. An interesting difference between the two methods was found and is shown in Fig. 2. The Ramsauer signal is seen to be relatively independent of accelerating voltage over a variation of about 7%, while the Brode signal is markedly peaked with accelerating voltage. This type of plot was made at various

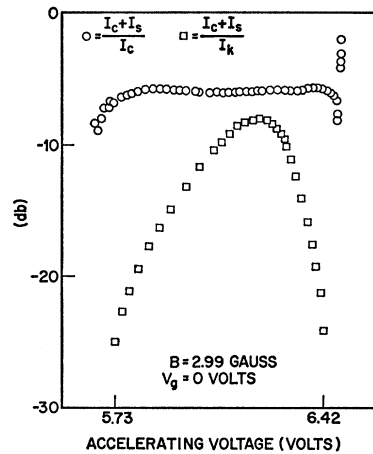


FIG. 2. A comparison between Ramsauer and Brode methods.

<sup>26</sup> Equation (4) assumes that  $F_0$  is a constant. This may not be true because of: (1) gas-cathode interactions, if differential pumping is not used; (2) minor drifts in the heater supply, accelerating supply, grid supply, or magnetic field.

energies and always showed the same general result: The Ramsauer signal was always independent of accelerating voltage over a range of about 7%, while the Brode signal was always markedly peaked. This result may be generalized to say that any small changes in accelerating voltage, grid voltage, or magnetic field strength make large changes in the Brode signal, while corresponding changes make only small changes in the Ramsauer signal. Actually, Brode- and Ramsauer-type measurements yielded the same results, except that Ramsauer-type results were much more reproducible. Furthermore, owing to space charge and field penetration into the energy selection region from the cathode region, the virtual cathode may exist in the selection region which would give an uncertainty in the path length for Brode-type measurements. For these reasons, and in order to use differential pumping to eliminate cathode cooling effects, the rest of the discussion will be concerned with Ramsauer-type measurements.<sup>26</sup> Although Ramsauer measurements at constant electron energy with and without the differential pumping yielded the same results, those with the differential pumping showed less scatter.

The energy  $E$  of an electron at a fixed radius  $r$  in a uniform magnetic field  $B$  is given by

$$E = (Ber)^2/2m, \quad (5)$$

where  $e$  and  $m$  are the electronic charge and mass, respectively. Hence, it would appear at first sight, that in an experiment such as this the measurement of energy would be accomplished by a straightforward measurement of magnetic field. Actually, the beam energy could be varied at constant magnetic field by varying the accelerating voltage and/or the grid cathode voltage, because of finite slit sizes. Furthermore, some of the welding near the outside of the apparatus was slightly magnetic, and magnetic-field measurements did not give reproducible energy measurements. This effect was stronger at the lower fields where the energy was not reproducible to better than 2% for constant-magnetic-field measurements. Hence, in order to avoid the problem of accurate knowledge of the relationship between magnetic-field strength and energy, as well as the annoyance of hysteresis in the magnet, retarding potential measurements on the beam were used to determine the electron energy.

Figure 3 shows a plot of a portion of a current versus retarding-potential curve in vacuum, and the energy distribution obtained therefrom by graphical differentiation. The data were taken by applying the retarding potential to both the scattering chamber and the collector and summing the two currents. This gave the energy distribution of the beam entering the scattering chamber. Energy distributions of the beam leaving the scattering chamber could be studied by holding it at ground potential and applying a retarding potential only to the collector. Because of the larger size of slits 5 and 6,

field penetration into the scattering chamber caused these retarding potential curves to be more rounded on top, but otherwise the two results were the same at higher energies. At quite low electron energies, the two distributions were not always identical and often retarding potential curves were taken both ways to study the behavior of the beam. When there was any difference in the energy distributions, the one taken with the retarding potential applied to the collector only was used. This was done because those electrons which enter the collector at zero pressure are the ones which would be scattered if gas were introduced.

The total energy spread of the beam  $\Delta E$  as determined by the slit system is roughly given by Eq. (5) to be

$$\Delta E/E \approx 2\Delta r/r, \quad (6)$$

where  $\Delta r$  is the slit width. For the present experiment this yields  $\Delta E/E$  between 6 and 7%, which might be expected to give a spread at half-maximum of about 3.5%. However, for sufficiently large values of  $E$ , the spread should become independent of  $E$  because the value of  $\Delta E$  which the slits will accept becomes larger than the available spread leaving the cathode.

The retarding potential measurements yielded widths at half-maximum of about 3% for energies from 1.5 to about 3 eV. For higher energies, the measured half-widths were indeed less than 3% of the energy. The resolution of the resonance at 19.3 eV, which is shown in Fig. 7, indicates a half-width of about 0.1 eV. The measured half-widths are consistent with the hypothesis that at higher energies the half-width was limited to about 0.1 eV by the spread in energies available from the cathode, but that an additional apparent spread of about 1% was caused by penetration of the retarding field through slit  $S_3$ . At lower energies, this error was negligible compared to actual beam width, and the measured widths are probably correct. For energies below 1.5 eV, when presumably a virtual cathode existed in front of  $S_1$ , the half-widths became 5 to 10% of the energy.

The general procedure for the cross-section measure-

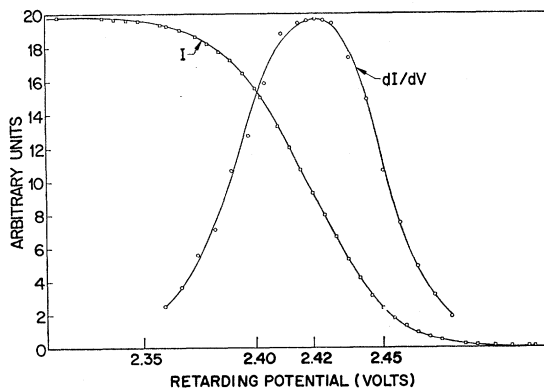


FIG. 3. A typical retarding-potential plot.

ments was the following. The magnetic field was set to obtain approximately the desired energy. The accelerating potential was adjusted, usually for a maximum in collector current, and the grid potential was adjusted to control the magnitude of current. (If a precise setting of electron energy was needed, the field and potentials could be readjusted as indicated by retarding potential measurements.) When all of the adjustments had been made, a retarding potential curve was plotted in order to measure the electron energy. After that,  $\ln I$  was measured and plotted, using a character printer, at various values of pressure increasing from zero to some maximum value.<sup>27,28</sup> The pressure was then decreased in a series of steps back to zero. Usually 15 to 20 different pressures were plotted for each run. If the data indicated that  $F_0$  had drifted during a run, that run was discarded.<sup>26</sup> Sometimes retarding-potential measurements were repeated<sup>29</sup> after a run in order to be sure that the energy had not changed during the run. Periodically, electrometer and pressure readings were recorded and  $\sigma_t$  was calculated from hand-plotted data in order to check the electronic system.

When the above procedure was followed, reproducible results were obtained for electron energies above about 1.4 eV. For lower energies, the results showed a scatter that increased rapidly with decreasing energy, until it was found that the condition of stability shown in Fig. 2 was not always obtained even for the Ramsauer measurements. Apparently, even the relatively low pressure of helium at the cathode could change the potential of the emitting surface, because when  $F_0$  could be made independent of accelerating potential, reproducible results were obtained. It was found that at higher energies the negative grid potentials used had automatically assured that  $F_0$  was independent of accelerating potential. At lower energies, with positive grid potentials relative to the cathode, it became increasingly difficult to find a combination of accelerating and grid potentials that would satisfy this condition because the range of accelerating voltage over which the Ramsauer signal remains independent of accelerating voltage decreases with decreasing energy. In fact, this placed the limit for the lowest energies studied. There was still a measurable current for energies below 0.2 eV, but, below 0.3 eV,  $F_0$  could not be made independent of accelerating potential.

## RESULTS

Values of  $\ln I$  were measured and plotted as a function of gas pressure at various constant values of electron

<sup>27</sup> The helium used throughout this work was Matheson assayed reagent grade gas in 1.1-liter Pyrex flasks. A complete analysis supplied by the manufacturer showed no detectable impurities of greater than 4 ppm by volume.

<sup>28</sup> Maximum pressure used in the scattering region was usually about 30  $\mu$ . With differential pumping maximum pressure at the cathode was roughly 7  $\mu$ .

<sup>29</sup> Retarding-potential measurements on the electron beam in the presence of gas at operating pressures yielded the same shape and energy spread as measurements in vacuum.

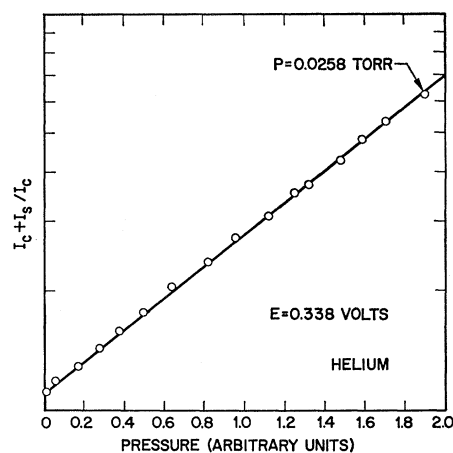


FIG. 4. A typical Ramsauer signal versus pressure plot.

energy, using the procedure outlined above. A typical example of such a plot is shown in Fig. 4 for an electron energy of 0.338 eV. From a measurement of the slope of this plot, the total cross section was determined to be  $5.30 \pm 0.04 \text{ \AA}^2$ . From many plots similar to Fig. 4 but at various different values of electron energy, the total cross section was determined as a function of electron energy for the range of electron energies between 0.300 and 28.0 eV. The resulting values of total cross section are plotted versus electron energy in Fig. 5 for three different gas samples of spectroscopically pure helium<sup>27</sup> and two different pressure gauges. The earlier direct measurements, of Ramsauer,<sup>1</sup> Ramsauer and Kollath,<sup>9</sup> Brode,<sup>2</sup> and Normand,<sup>10</sup> as well as the calculations of Morse and Allis<sup>7</sup> are also shown on the plot. It is to be noted that no low-energy "fine structure" has been

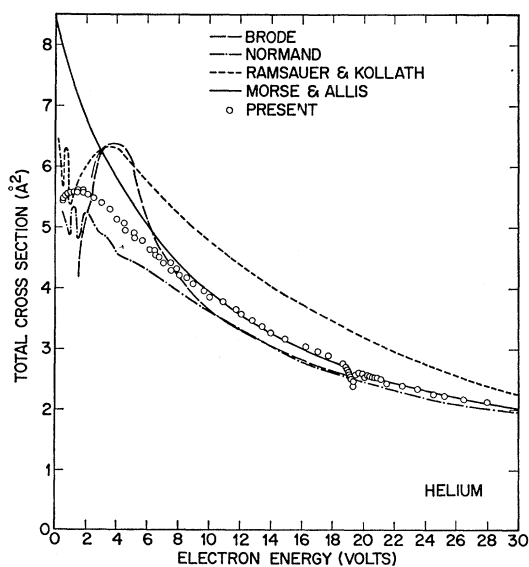


FIG. 5. Total electron-helium-atom cross section versus energy 0-30 eV.

found in the present experiment. Neglecting the detailed variation of cross section with electron energy, the cross section is seen to first increase with decreasing electron energy from  $2.2 \text{ \AA}^2$  at  $28.0 \text{ eV}$  to a maximum of  $5.6 \text{ \AA}^2$  at about  $1.2 \text{ eV}$ , and then decrease to  $5.4 \text{ \AA}^2$  at  $0.300 \text{ eV}$ . At the higher electron energies, the present measurements are in very good agreement with the calculations of Morse and Allis.<sup>7</sup> However, as the electron energy is decreased for energies below about  $7 \text{ eV}$ , the present results deviate more and more from their calculations. Whereas the present measurement at  $6 \text{ eV}$  is about  $6\%$  lower than their calculation, the present measurement at  $1 \text{ eV}$  is about  $30\%$  lower than their calculation. This discrepancy between the experiment and the calculation at the lower energies is to be expected due to the neglect of the polarization and distortion in the calculation of Morse and Allis. The introduction of such corrections into the calculation would have the effect of bringing the calculated cross section down at the lower electron energies.<sup>20,30</sup> The present results are about  $6\%$  higher than those of Normand<sup>10</sup> at the higher electron energies. If the "fine structure" found by Normand at the lower electron energies is neglected and averaged out, the present measurements are about  $10$  to  $12\%$  higher than his. Normand<sup>10</sup> used essentially the same apparatus as Brode.<sup>2</sup> Brode's measurements are in very good agreement with those of Normand for energies greater than about  $7 \text{ eV}$ . However, for lower electron energies, Brode's measurements deviate by as much as  $50\%$  from those of Normand. Brode's results have a peak at about  $4 \text{ eV}$ , which is  $50\%$  higher than the measurement of Normand at  $4 \text{ eV}$ . As the energy is decreased below  $4 \text{ eV}$ , Brode's results drop abruptly to about  $25\%$  below the results of Normand at about  $1.5 \text{ eV}$ . The present measurements are about  $15$  to  $20\%$  lower than the results of Ramsauer and Kollath,<sup>1,9</sup> except at the lower electron energies, where if again the "fine structure" is averaged out, the present results are about  $7\%$  lower than theirs.

The present measurements for electron energies less than  $4 \text{ eV}$  are shown in Fig. 6 on expanded scales. The other direct measurements of Ramsauer and Kollath<sup>1,9</sup> and Normand<sup>10</sup> are also shown. The values of the cross section for momentum transfer given by Gould and Brown<sup>12</sup> are shown on the plot as triangles with their estimated error bars at the highest energy at which they made a measurement as well as at their extrapolated zero-energy value. The other indirect measurements of the cross section for momentum transfer shown are the measurements of Frost and Phelps<sup>16</sup> shown as the upper dashed line. It should be noted that total and momentum transfer cross-section measurements may be compared only if the scattering is isotropic. The solid line going through the present data points is the best fit to the present data using the effective range formula given by

<sup>30</sup> R. W. LaBahn and J. Callaway, Phys. Rev. **135**, A1539 (1964).

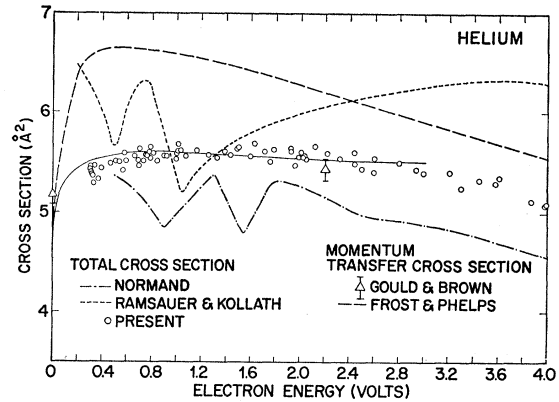


FIG. 6. Total electron-helium-atom cross section versus energy 0-4 eV.

O'Malley<sup>20</sup> between  $0.30$  and  $3.0 \text{ eV}$  and extrapolating to zero eV. The following formula was fitted to the data using the method of least squares<sup>31</sup>:

$$\sigma_t(\text{\AA}^2) = A + 1.4484\sqrt{A}\sqrt{E} + 0.13333AE \ln E - BE, \quad (7)$$

where  $\sigma_t$  is the total scattering cross section in  $\text{\AA}^2$ ,  $A = 4\pi a^2$ ,  $a$  is the scattering length,  $E$  is the electron energy in electron volts. In Eq. (7), the polarizability has been assumed to be  $(\alpha = 1.36a_0^3)$ ,<sup>32</sup> where  $a_0 = 0.529 \text{ \AA}$ .

The values of the various parameters obtained by the best fit to the data as given by Eq. (7) are given in Table I. The value of scattering length of  $1.15a_0$  obtained from the present work is in good agreement with the recent value obtained by Frost and Phelps<sup>16</sup> of  $1.18a_0$ . Equation (7) was also fitted to the data with the polarizability increased by about  $10\%$ <sup>33</sup> to test whether or not this experiment offered a measure of the polarizability of helium. The resulting values are given in Table I. However, the fit was essentially the same as that obtained with  $\alpha = 1.36a_0^3$ . It was concluded that the present measurements do not extend to sufficiently small values of  $E$  in order to give a sensitive measure of  $\alpha$ .

The remaining feature of the present measurements is the sharp resonance at about  $19.3 \text{ eV}$  which was

TABLE I. Values of the parameters for the modified effective-range formula.

$\alpha$	$A$	$B$	$a$
$1.36a_0^3$	4.680	2.225	$1.15a_0$
$1.49a_0^3$	4.604	2.415	$1.14a_0$

<sup>31</sup> Actually, the sum of the squares of the percentage differences between measured and calculated values of  $\sigma_t$  was minimized by variation of the parameters  $A$  and  $B$  in Eq. (7).

<sup>32</sup> J. H. Van Vleck, *The Theory of Electric and Magnetic Susceptibilities* (Clarendon Press, Oxford, England, 1932).

<sup>33</sup> E. G. Wikner and T. P. Das, Phys. Rev. **107**, 497 (1957).

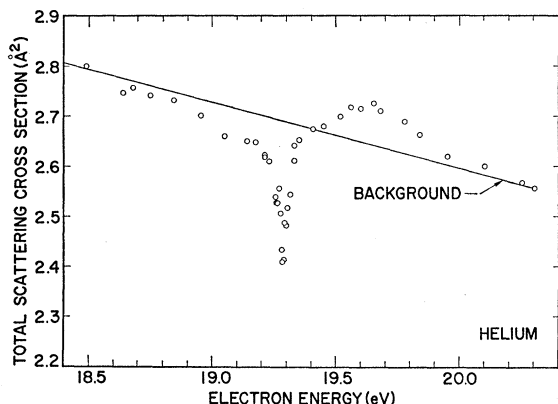


FIG. 7. Total electron-helium-atom cross section versus energy in the vicinity of the resonance.

postulated by Baranger and Gerjuoy<sup>34</sup> and first observed by Schulz<sup>35</sup> as a decrease in the scattering to a fixed scattering angle. Figure 7 shows the present results for the total cross section near the resonance as a function of electron energy on an expanded scale. The solid line represents the scattering cross section in the absence of the resonance. The observed resonance width is a good measure of the beam width at that energy because the actual resonance width must be very much narrower than observed. The resonance width is probably about 0.01 eV as has been estimated by Simpson and Fano.<sup>36</sup> The minimum at  $19.285 \pm 0.025$  eV is about 10% below the background, and the maximum at  $19.65 \pm 0.05$  eV is about 3% above the background.

#### DISCUSSION

The rather large discrepancies between various results, and the observed structure<sup>9,10</sup> at low energies have not really been explained. O'Malley<sup>20</sup> has suggested that the "fine structure" in the results of Ramsauer and Kollath could be attributed to the presence of a few percent of  $N_2$  and  $O_2$ . In the early stages of the present work, the data showed a rather large peak and some fine structure with a fair degree of reproducibility. Further work reduced this to a large scatter which disappeared after establishing the criterion that  $F_0$  must first be made independent of accelerating potential. The initial reproducibility of structure may be attributed to habit. That is, when the experimenter wished to take data at a particular energy he was likely to follow about the same routine of setting the field; adjusting accelerating voltage for peak current, grid voltage to obtain a convenient current level, etc. It was only when adjustments were deliberately varied that the structure degenerated to scatter. Because of the different "electron guns" used in the other experiments, these observations may not apply to them, but they are suggestive.

<sup>34</sup> E. Baranger and E. Gerjuoy, *Phys. Rev.* **106**, 1182 (1957); *Proc. Phys. Soc. (London)* **A72**, 326 (1958).

<sup>35</sup> G. J. Schulz, *Phys. Rev. Letters* **10**, 104 (1963).

<sup>36</sup> J. A. Simpson and U. Fano, *Phys. Rev. Letters* **11**, 158 (1963).

As discussed earlier the electrometers were compared and calibrated to about  $\pm 0.3\%$  at their outputs, and the remainder of the electronics was checked to an accuracy of better than  $\pm 1\%$  by comparison with hand-plotted data. Adjustment of amplifier gain to make a 10 db change in  $\ln F$  fit the graph paper was performed for nearly every run, so should have contributed only to random scatter of the final data. Similarly, errors of reading the plots should be random:  $\pm 1\%$  should be a conservative estimate of over-all systematic errors for measuring and processing the data on currents. Pressure measurements have been discussed above and contribute two independent errors of about  $\pm 1\%$  and  $\pm 2\%$ . In the Appendix it is argued that the probable error in detection of scattering should be about  $\pm 1\%$ . Taking  $\pm 1\%$  as a reasonable uncertainty in path length, we have five independent errors of about  $\pm 1\%$  and one of  $\pm 2\%$ . Although two of these should be upper limits of error, if we treat them all as probable errors we have an over-all estimate probable error of  $\pm 3\%$ .

#### ACKNOWLEDGMENTS

The authors wish to thank the members of the Physical Electronics Group for many helpful discussions.

#### APPENDIX: THE GEOMETRIC ANGULAR DETECTION EFFICIENCY

If experimental errors are neglected, the apparatus still does not measure the total scattering cross section exactly, because some of the electrons scattered to small angles may pass through the slits. It is a difficult problem to calculate this detection error for the curved geometry in the magnetic field, but something can be learned from a study of a simplified linear model.

Consider first the simple two-dimensional problem of scattering to some angle  $\theta$  between 0 and  $\pi/2$  from a linear beam element of length  $L$  which passes a distance  $r$  from a slit edge, as depicted in Fig. 8. Scattering events occurring at positions  $r/\tan\theta \leq z \leq L$  are detected, but events occurring at  $z < r/\tan\theta$  are not detected. Then, of all the electrons scattered to the angle  $\theta$  from the ele-

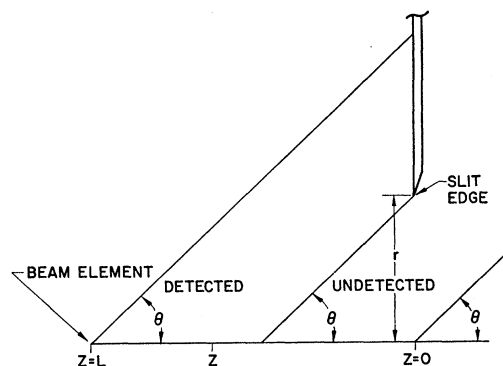


Fig. 8. Angular-scattering detection by a one-dimensional slit for a one-dimensional monoenergetic beam.

ment of length  $L$ , the fraction that is detected (neglecting beam attenuation) is given by

$$f(\theta) = 1 - r/L \tan\theta.$$

This result has been generalized to the problem of a linear, monoenergetic beam with uniform current density, and a rectangular cross section equal to that of the exit slit, assuming azimuthally isotropic scattering. The solution is a rather lengthy one which gives four expressions for  $f(\theta)$  for four ranges of  $\theta$  depending on the slit dimensions. For the sake of brevity, only the results are presented in Fig. 9 for three specific cases. The dimensions (path length of beam in the scattering region, and slit dimensions) of the present apparatus, Ramsauer and Kollath's<sup>9</sup> apparatus, and Brode<sup>2</sup> and Normand's<sup>10</sup> apparatus have been used as dimensions of the linear system. In the Brode method, a back-scattered electron would be undetected only if it returned to the cathode, so  $f(\theta) = 1$  for  $90^\circ \leq \theta \leq 180^\circ$ . For the present apparatus, the curve is asymmetrical because the entrance slit to the scattering region is much smaller than the exit slit from it.

It is difficult to determine whether the detection for the circular beam is better or worse than for the idealized linear system. It is our opinion that there is probably not much difference. Back-scattered electrons which escape out of the entrance slit of the scattering region are lost from the measurement of both  $I_0 = I_{s0} + I_{e0}$  and  $I_c$ . Instead of being counted as unscattered, they are not counted at all. However, the detection errors for both forward and backward scattering are second order effects. Nondetection of small-angle forward scattering into the collector is in part canceled by large-angle scattering from the collector back into the scattering region. Similarly, small-angle scattering from the beam in front of the scattering chamber can enter the scattering chamber to be counted as scattered current. Actually, for isotropic scattering, the net error is to measure too much scattering due to beam attenuation and back-scattered electrons which escape out of the entrance to the scattering region.

Assuming isotropic scattering, when  $f(\theta)$  (as plotted in Fig. 9 for dimensions of the present experiment) is multiplied by  $\sin\theta$  and integrated over  $\theta$ , it is found that the calculated loss of detection of small-angle scattering is 3.6% of the total scattering, and the loss

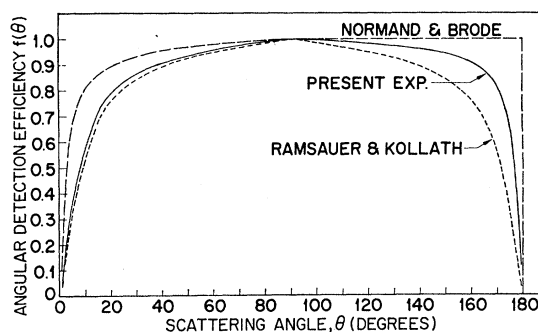


FIG. 9. Angular-scattering detection efficiency by a two-dimensional slit for a linear monoenergetic beam of rectangular cross section.

to back scattering at the entrance slit is 1.6%. Assuming only 75% cancellation by the opposite effect at each end reduces these to 0.9 and 0.4%, respectively. Further, these figures are for no attenuation of the beam; when the beam is attenuated as the pressure is increased the error due to loss of detection at the exit slit is correspondingly reduced. Remembering also that the net errors at entrance and exit are of opposite sign, the over-all net error would be no more than a few tenths of a percent for isotropic scattering.

For helium, LaBahn and Callaway<sup>30</sup> predict strong asymmetry in the backward direction at low energies and in the forward direction at high energies, with crossover somewhere about 15 eV. This alters the cancellation effects at the entrance and exit slits. Judging from their plots of differential cross section compared to plots of our calculated detection error, the cancellation might fall to roughly 25% at 2.5 and 21 eV. This leaves calculated errors at exit and entrance slits of 2.7 and 1.2% of the total, respectively, at the limit of zero pressure. At high energies, with maximum beam attenuations of about 60%, the effect of the error at the exit slit would be reduced from 2.7 to  $\approx 1\%$ ; the net calculated error would then be negligible. At low energies and high cross sections, beam attenuations up to 85% would reduce the error at the exit slit to  $\approx 0.4\%$  leaving a net error of  $\approx 0.8\%$ .

Considering the above, our best estimate of the probable error in the cross section measurement due to detection error is about  $\pm 1\%$  for the whole energy range studied.